

Northumbria Research Link

Citation: Li, Xiang, Zhu, Yaofeng, Liu, Xuqing, Xu, Bin and Ni, Qingqing (2020) A broadband and tunable microwave absorption technology enabled by VGCFs/PDMS–EP shape memory composites. *Composite Structures*, 238. p. 111954. ISSN 0263-8223

Published by: Elsevier

URL: <https://doi.org/10.1016/j.compstruct.2020.111954>
<<https://doi.org/10.1016/j.compstruct.2020.111954>>

This version was downloaded from Northumbria Research Link:
<http://nrl.northumbria.ac.uk/id/eprint/41932/>

Northumbria University has developed Northumbria Research Link (NRL) to enable users to access the University's research output. Copyright © and moral rights for items on NRL are retained by the individual author(s) and/or other copyright owners. Single copies of full items can be reproduced, displayed or performed, and given to third parties in any format or medium for personal research or study, educational, or not-for-profit purposes without prior permission or charge, provided the authors, title and full bibliographic details are given, as well as a hyperlink and/or URL to the original metadata page. The content must not be changed in any way. Full items must not be sold commercially in any format or medium without formal permission of the copyright holder. The full policy is available online: <http://nrl.northumbria.ac.uk/policies.html>

This document may differ from the final, published version of the research and has been made available online in accordance with publisher policies. To read and/or cite from the published version of the research, please visit the publisher's website (a subscription may be required.)



UniversityLibrary



Northumbria
University
NEWCASTLE

Manuscript Details

Manuscript number	COST_2019_3916_R1
Title	A broadband and tunable microwave absorption technology enabled by VGCFs/PDMS–EP shape memory composites
Article type	Full Length Article

Abstract

A facile method for fabricating intelligent microwave absorber of vapor grown carbon fibers/Polydimethylsiloxane–epoxy resin shape memory composites (VGCFs/PDMS–SMEP) composites was proposed to deliver intelligently tunable and broadband microwave absorption performance. The maximal absorption intensity was regulated by varying the deformation of the composites driven by the superior shape memory property of SMEP, where practical the minimum reflection loss (RL_{min}) reaches -55.7 dB at 16.0 GHz with the thickness of 2.0 mm. The effective absorption bandwidth (EAB) reached 9.8 GHz, which covered the whole applied frequency range (8.2–18.0 GHz). The intelligent microwave absorption performance of the sample was attributed to robust conductive loss and dielectric loss enhanced by the dipole relaxations and multi-reflections. Thus, VGCFs/PDMS–SMEP composites serves as the key that really opens up opportunity for the application as flexible, shape memory and tunable high performance broadband microwave absorption absorber in frontiers such as wearable electronic devices, chips protection, stealth technology and information security.

Keywords Tunable microwave absorption, frequency regulation, shape memory, wearable microwave absorber, VGCFs/PDMS

Corresponding Author Yaofeng Zhu

Corresponding Author's Institution Zhejiang Sci-Tech University

Order of Authors Xiang Li, Yaofeng Zhu, Xuqing Liu, BEN XU, Qing-Qing Ni

Suggested reviewers Yaqin Fu, Fanbin Meng, Shao-Yun Fu

Submission Files Included in this PDF

File Name [File Type]

Cover letter.docx [Cover Letter]

Response to Reviewers.docx [Response to Reviewers]

Highlights.docx [Highlights]

Mark-up Revised Manuscript.docx [Manuscript File]

Declaration of competing interests.docx [Conflict of Interest]

Author Statement.docx [Author Statement]

Supporting Information.docx [e-Component]

To view all the submission files, including those not included in the PDF, click on the manuscript title on your EVISE Homepage, then click 'Download zip file'.

1 **A broadband and tunable microwave absorption technology enabled by**
2 **VGCFs/PDMS–EP shape memory composites**

3 Xiang Li^a, Yaofeng Zhu^{a*}, Xuqing Liu^b, Ben Bin Xu^{c*}, Qingqing Ni^d

4 ^a *Key Laboratory of Advanced Textile Materials and Manufacturing Technology of Ministry*
5 *of Education, Zhejiang Sci–Tech University, No. 928 Second Avenue Xiasha Higher*
6 *Education Zone, Hangzhou, 310018, Zhejiang, P.R. China*

7 ^b *School of Materials, University of Manchester, Oxford Road, Manchester, United Kingdom,*
8 *M13 9PL*

9 ^c *Department of Mechanical and Construction Engineering, Northumbria University,*
10 *Newcastle upon Tyne, United Kingdom, NE1 8ST*

11 ^d *Interdisciplinary Graduate School of Science and Technology, Shinshu University, Tokida,*
12 *Ueda, 386-8576, Japan*

13

14

15

16

17

18

19

20 *Corresponding authors.

21 *Email addresses: yfzhu@zstu.edu.cn (Y. Zhu), ben.xu@northumbria.ac.uk (B. Xu).*

22

1 **ABSTRACT**

2 A facile method for fabricating intelligent microwave absorber of vapor grown carbon
3 fibers/Polydimethylsiloxane–epoxy resin shape memory composites (VGCFs/PDMS–SMEP)
4 composites was proposed to deliver intelligently tunable and broadband microwave
5 absorption performance. The maximal absorption intensity was regulated by varying the
6 deformation of the composites driven by the superior shape memory property of SMEP,
7 where practical the minimum reflection loss (RL_{min}) reaches -55.7 dB at 16.0 GHz with the
8 thickness of 2.0 mm. The effective absorption bandwidth (EAB) reached 9.8 GHz, which
9 covered the whole applied frequency range (8.2–18.0 GHz). The intelligent microwave
10 absorption performance of the sample was attributed to robust conductive loss and dielectric
11 loss enhanced by the dipole relaxations and multi-reflections. Thus, VGCFs/PDMS–SMEP
12 composites serves as the key that really opens up opportunity for the application as flexible,
13 shape memory and tunable high performance broadband microwave absorption absorber in
14 frontiers such as wearable electronic devices, chips protection, stealth technology and
15 information security.

16

17 **Keywords:** Tunable microwave absorption, frequency regulation, shape memory, wearable
18 microwave absorber, VGCFs/PDMS.

1 **1. Introduction**

2 With the significant advance in recent development of portable electronic devices, high-
3 performance microwave absorption materials (MAMs) [1,2] with broadband and tunable
4 microwave absorption (MA) capabilities is highly demanded to address the challenges such
5 as to protect electronic devices and absorb adverse electromagnetic waves [3,4]. The
6 conventional microwave absorption strategy is to apply solid powdered absorbers, *i.e.* ferrites,
7 ceramics, carbon materials and their hybrids as coatings or fillers into matrices to fulfill the
8 microwave absorption functions [5,6], which is normally fixed on certain microwave
9 broadband and less adaptive to respond to the changes of microwave direction due to
10 structural limitation (coating thickness) of absorber [7].

11 To address above challenges, some attempts have been made to achieve tunable MA
12 performance by chemically or physically adjusting electromagnetic parameters [8], realigning
13 the absorbers to improve impedance matching characteristic [9], changing the moisture
14 content [10] and controlling the thickness of absorbing layer to broaden the effective
15 absorption bandwidth (EAB) [11], etc. However, these practices haven't resolved the
16 drawbacks, such as non-adaptivity for smart MA, low integrability to scale-up production,
17 and poor stability, therefore, microwave absorbing technology with tunable and broadband
18 MA performance remains yet to be fully explored [12].

19 **Shape memory polymer (SMP) can be activated by various external stimuli, such as**
20 **thermal, electric, light, and pH, etc [13–16], where structure geometry can be tuned and**
21 **programmed via designing a shape recovery performance [17].** Comparing with the
22 conventional absorbers with fixed loading ratio, extra controllability can be achieved by this

1 autonomous recovery feature of SMP to regulate the MA performance [4]. Such continuous
2 shape deformation ability of SMP endows its' geometrical effect, which facilitate SMP to be
3 used as intelligent MAMs to respond to electromagnetic waves with diverse frequencies. To
4 date, the efforts to enable microwave absorber with tunable MA properties by using SMPs,
5 haven't reported elsewhere.

6 Herein, we fabricated a VGCFs/PDMS-SMEP composites structure consisting of
7 broadband and tunable high microwave absorbing performance. Empowered by shape
8 memory effect, the VGCFs/PDMS-SMEP composites exhibits state-of-the-art tunable MA
9 ability. The maximal absorption capability was well-regulated by programming the
10 deformation of composites under thermal stimuli, where we achieve a broad EAB covering
11 the whole testing frequency range of 9.8 GHz (8.2-18 GHz). We anticipate this shape
12 recovery based autonomous microwave absorption structure to find future applications in
13 wearable devices, chips protection, and information security.

14 **2. Experimental section**

15 **2.1. Materials:**

16 Commercially available water-borne epoxy resin (WEP, AB-EP20 emulsion, 50% solid
17 content) and amine based waterborne curing agent (AB-HGF) were purchased from Zhejiang
18 An bang New Material Development Co., Ltd, China. Vapor grown carbon fiber (VGCF,
19 Showa Denko K.K., Japan) was fabricated by thermo-chemical vapor deposition.
20 Polydimethylsiloxane (PDMS) was obtained from Shenzhen Hongyejie Technology Co. Ltd.
21 Ultra-pure water were obtained from commercial sources. All reagents were used as obtained
22 without further purification.

1 **2.2. Fabrication of shape memory epoxy sheet:**

2 Shape memory epoxy sheet (SMEP) was fabricated based on our previous reported work
3 [16]. Briefly, water-borne epoxy resin and amine based waterborne curing agent were mixed
4 to homogeneity at room temperature under vigorously stirring, where the weight ratio of
5 WEP to curing agent was 4:1. Then, the above mixture was frozen in liquid nitrogen, and
6 subsequently dried in a Labconco Free Zone freeze-drier operated at 0.1 mbar and -15°C for
7 two weeks. Finally, the resulting compound powder was compressed into sheet (25 cm*18
8 cm length by width) at 120°C under a pressure of 10 MPa for 2 h. The resulting shape
9 memory epoxy sheet was obtained with the thickness approximately 0.5 mm.

10 **2.3. Fabrication of VGCFs/PDMS-EP shape memory composites:**

11 Different weight of VGCFs (2 g, 4 g, and 6 g) was added to 40 g liquid PDMS with
12 continuously stirring for 30 min to uniformly dispersed, respectively. The mixture was
13 poured into a 260*190*2 mm mold (L*W*H), then the as-prepared SMEP was immersed into
14 the liquid VGCFs/PDMS mixture. Finally, VGCFs/PDMS-EP shape memory composites
15 were obtained after curing 6 h under a pressure of 5 MPa at room temperature.

16 **2.4. Thermal mechanical cycle test:**

17 A thermo-mechanical analyzer (TMA, TA Instruments Q400) was used to measure the
18 shape memory properties of VGCFs/PDMS-EP shape memory composites under dynamic
19 DMA mode. The sample was stretched with an increasing stress from 0 to 0.3 MPa at 80°C ($>$
20 T_g). Then, it was stretched isothermally with a constant force of 0.3 MPa for 5 min. The
21 sample was subsequently cooled down to 20°C ($< T_g$) to fix the temporary shape with the
22 external force, after which the load was released at 20°C (the loading and unloading speed

1 was 0.1 MPa/min). Then, the samples were heated from 20°C to 80°C without load and held
2 for 10 min, resulting in the recovery of the samples' strain. A residual strain would remain
3 when this cycle was finished. The heating or cooling speed was 10 °C/min.

4 **2.5. Practical microwave absorption performance from arch method measurement:**

5 In the measurement of practical performance, the as-fabricated artificial sandwich
6 structures (250 × 180 mm² in planar size) were placed on the holder of the arch setup. In the
7 investigation region from 8.2 to 18 GHz, the setup was performed on VNA (N5222A,
8 Keysight).

9 **2.6. Waveguide measurement for complex permittivity:**

10 VGCFs/PDMS-EP shape memory composite was cut into 10×20 mm, and the
11 electromagnetic parameters were measured by VNA measurement working in the frequency
12 range of 8.2–12.4 GHz.

13 **2.7. Characterization**

14 The morphology of samples was observed by scanning electron microscopy (FE-SEM,
15 Ultra55, Zeiss, Germany). Fourier transform infrared spectroscopy (FT-IR) is recorded on a
16 Nicolet 5700 FT-IR spectrometer. The crystal structure was characterized by X-ray
17 diffraction (Bruker AXS D8-Discover, Cu-K α radiation). The shape memory performance of
18 the composite was conveniently measured by thermal-mechanical cycle tests conducted on
19 the TMA Q400 (TA Instruments), and tensile mechanical property was measured by Instron
20 3367 tensile test instrument (USA) at 25±1°C room.

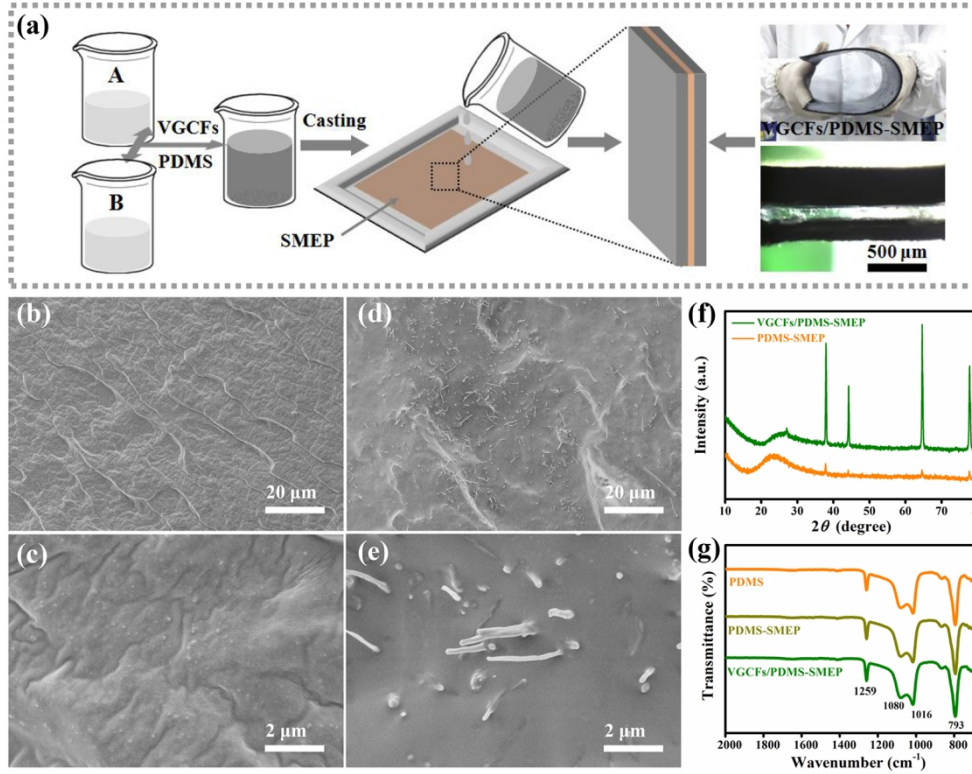
21

1 3. Results and discussion

2 3.1. Structures of VGCFs/PDMS–SMEP composites

3 The preparation of VGCFs/PDMS–SMEP composite structure is illustrated in Fig. 1a.
4 SMEP was firstly obtained by frozen drying and thermal compression method with the length
5 by width of 25 cm*18 cm. Different amount of VGCFs (microwave absorb component [18])
6 were added into liquid PDMS for mixing and poured into casting mold to form
7 VGCFs/PDMS–SMEP composite. The cross-section FE–SEM images in Fig. S2 identify an
8 uniform distribution of VGCFs in PDMS at a loading ratio of 10 wt%. For pristine PDMS,
9 the cross section view shows wrinkled structure (Fig. 1b, c). However, the wrinkled surface
10 turned into smooth after hybridized with VGCFs (Fig. 1d, e), indicating the formation of
11 dense structure [16].

12 The XRD pattern of PDMS–SMEP spike four weak peaks at 38°, 44.2°, 64.6°, and 77.8°,
13 representing the low crystallization of silicon rubber [19,20]. For VGCFs/PDMS-SMEP
14 composites, the structure of PDMS was well-maintained, with a new peak at 27° emerged to
15 show the intrinsic ordered crystal structure of VGCFs [21]. FT–IR spectrum (Fig. 1g)
16 suggested peaks at 1080 cm⁻¹ and 1016 cm⁻¹ for Si–O–Si asymmetrical stretching vibration,
17 peaks at 1259 cm⁻¹ and 793 cm⁻¹ for the stretching vibration of Si–CH₃ and the blending of
18 C–H in the chain segments of PDMS [22].



1
 2 **Fig. 1.** (a) Schematically illustration of synthesis process and cross section polarizing
 3 microscope image of VGCFs/PDMS–SMEP composite. Cross section FE–SEM images of
 4 PDMS (b) low resolution and (c) high resolution, VGCFs/PDMS (d) low resolution and (e)
 5 high resolution, respectively. (f) XRD patterns, and (g) FT–IR spectra of as–fabricated
 6 samples.

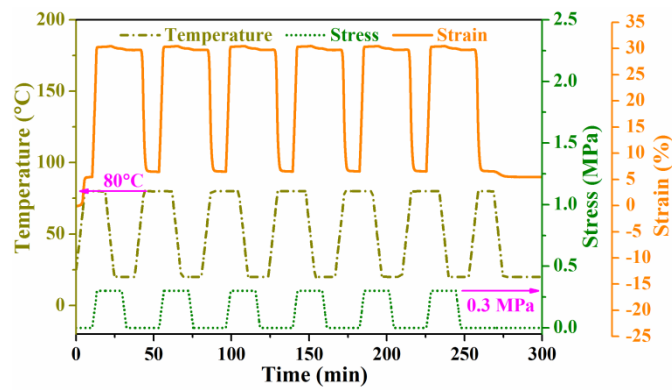
7 **3.2. Shape memory effects of VGCF/PDMS–SMEP composites**

8 Shape memory performance of VGCF/PDMS–SMEP composites can be evaluated by the
 9 shape fixity ratios (R_f , the capacity to maintain the temporary shape) and shape recovery
 10 ratios (R_r , the capacity to recover the initial shape), which can be expressed by the following
 11 equations [23]:

12
$$R_f = \frac{\varepsilon_f - \varepsilon_{f0}}{\varepsilon_m - \varepsilon_{f0}} \quad (1)$$

13
$$R_r = \frac{\varepsilon_f - \varepsilon_r}{\varepsilon_f - \varepsilon_{f0}} \quad (2)$$

1 Where ε_{f0} , ε_m , ε_f and ε_r are the strain of original, maximum elongated, fixing, and recovery,
 2 respectively. In the first cycle, the shape recovery ratio of composites is 95.0%. Interestingly,
 3 the shape recovery ratios of the composites rises to more than 99.0% after the second cycle
 4 (Fig. 2) [24]. The superior shape memory performance endorse the composites with
 5 reversible deformation and maintain a permanent shape, which is potential to be used as an
 6 intelligent microwave absorber.



7
 8 **Fig. 2.** Thermal mechanical cycles of VGCFs/PDMS-SMEP composites.

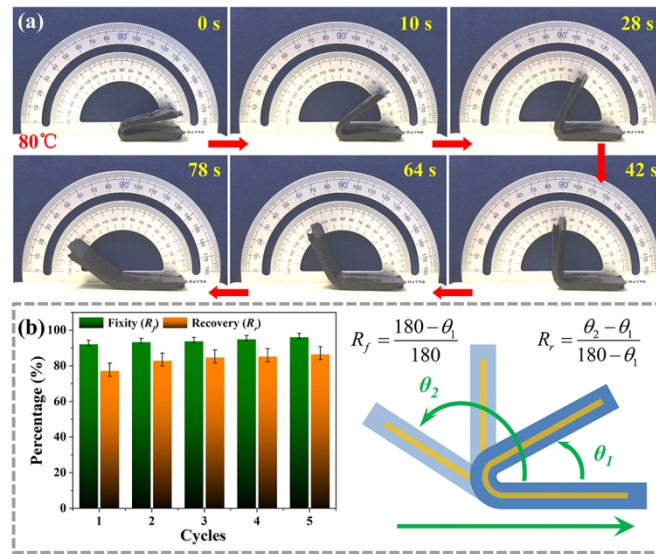
9 The shape recovery testing of VGCFs/PDMS-SMEP composites is performed at 80°C (Fig.
 10 3a), benefited from the excellent shape memory property, the sample can be recovered from a
 11 large bending deformation after being endowed with a temporary shape under thermal stimuli
 12 [25]. Furthermore, the shape fixity and recovery ratios of the sample are also calculated as the
 13 following equations [26]:

$$14 \quad R_f = \frac{180 - \theta_1}{180} \quad (3)$$

$$15 \quad R_r = \frac{\theta_2 - \theta_1}{180 - \theta_1} \quad (4)$$

16 Where θ_1 and θ_2 are degree of fixing and recovery, respectively, which are illustrated in Fig.
 17 3b. Both fixity and recovery of VGCFs/PDMS-SMEP show the obvious increase trend with

1 the cycles. The shape fixity and recovery ratio are maintained at 97% and 87% after several
 2 repeatedly deformation, respectively, which are lower than the calculated values from TMA
 3 instruments. This phenomenon is attributed to the large scale sandwich-like structure, where
 4 the thick elastic PDMS layer force SMEP back to initial state and decrease θ_l values, thus
 5 diminishing the shape fixity and recovery ratio of SMEP [16].



6
 7 **Fig. 3.** (a) Shape memory behavior of VGCFs/PDMS-SMEP composites at 80°C. (b)
 8 Calculated fixity and recovery of VGCFs/PDMS-SMEP composites.

9 3.3. Microwave absorption properties of VGCFs/PDMS-SMEP composites

10 The measured real part (ϵ') and imaginary part (ϵ'') of complex permittivity ϵ_r ($\epsilon_r = \epsilon' - j\epsilon''$),
 11 are determined for as-prepared samples in the frequency range of 8.2–12.4 GHz, where the ϵ'
 12 and ϵ'' represent the storage and loss of electric energy, respectively (Fig. 4a, b) [27]. For the
 13 VGCFs/PDMS-SMEP composites, the values of ϵ' , ϵ'' , and $\tan\delta_\epsilon$ are increased with the
 14 addition of VGCFs. Whereas to the as-prepared samples, the values of real part (μ') and
 15 imaginary part (μ'') of complex permeability μ_r ($\mu_r = \mu' - j\mu''$) are maintained at 1.0 and 0.0,
 16 respectively (Fig. S3), indicating that the MA of samples is mainly dependent on dielectric

1 loss [28]. In addition, it is found that several resonance peaks exist in the dielectric loss
 2 curves of VGCFs/PDMS–SMEP composites, implying the raise of multiple relaxation
 3 processes. Based on the Debye relaxation theory, the relaxation process can be analyzed by
 4 Cole–Cole semicircle (Fig. 4d–f), which is calculated by the following equations [6]:

$$5 \quad \varepsilon_r = \varepsilon' - j\varepsilon'' = \varepsilon_\infty + \frac{\varepsilon_s - \varepsilon_\infty}{1 + j2\pi f\tau} \quad (5)$$

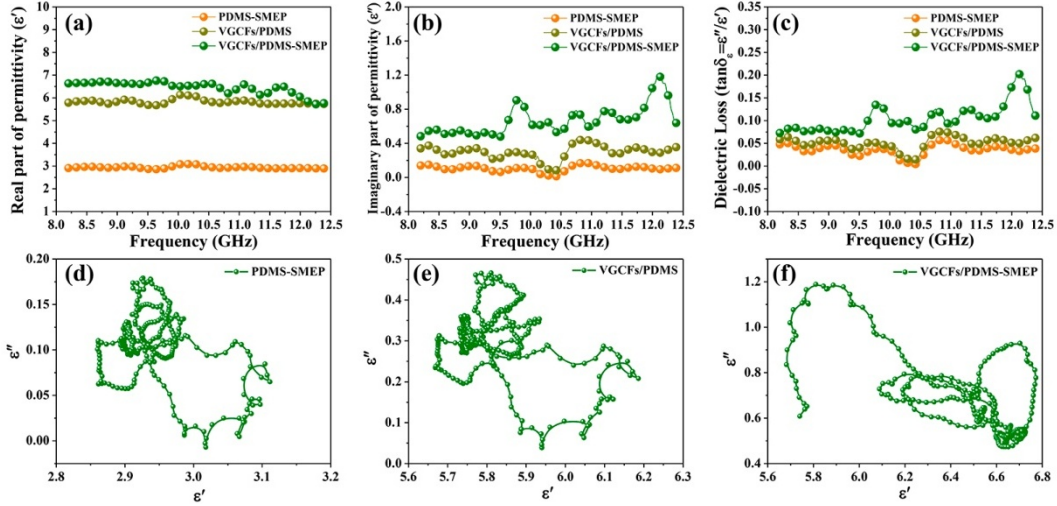
$$6 \quad \varepsilon' = \varepsilon_\infty + \frac{\varepsilon_s - \varepsilon_\infty}{1 + (2\pi f\tau_0)^2} \quad (6)$$

$$7 \quad \varepsilon'' = \frac{\omega\tau_0(\varepsilon_s - \varepsilon_\infty)}{1 + (2\pi f\tau_0)^2} \quad (7)$$

8 Where f , τ_0 , ε_s and ε_∞ are the frequency, relaxation time, static dielectric constant and
 9 dielectric constant at infinite frequency, respectively. Equation (2) and (3) were deduced from
 10 equation (1) and the relationship between ε' and ε'' was further deduced from equation (2) and
 11 (3), which are given below:

$$12 \quad \left(\varepsilon' - \frac{\varepsilon_s + \varepsilon_\infty}{2}\right)^2 + (\varepsilon'')^2 = \left(\frac{\varepsilon_s - \varepsilon_\infty}{2}\right)^2 \quad (8)$$

13 From equation (8), the curves of ε' and ε'' form single semicircle, each of which contributes to
 14 one Debye relaxation process. In Fig. 4d and e, PDMS–SMEP and VGCFs/PDMS possess
 15 similar curves variation trend, which simultaneously immersed several Debye–like relaxation
 16 processes. Moreover, VGCFs/PDMS–SMEP composites displayed more regular Cole–Cole
 17 semicircles, revealing the presence of more Debye polarization relaxation processes (Fig. 4f),
 18 which coincided with the results of dielectric loss in Fig. 4c. Hence, the addition of VGCFs
 19 and construction of sandwich–like structure of the composites enhanced dielectric loss in the
 20 form of multiple relaxation processes [11].



1
2 **Fig. 4.** (a) Real part and (b) imaginary part of complex permittivity and (c) dielectric loss of
3 samples, typical Cole-Cole semicircle of (d) PDMS-SMEP, (e) VGCFs/PDMS and (f)
4 VGCFs/PDMS-SMEP (filler loading of 10 wt% with VGCFs).

5 Microwave absorption property represented by reflection loss (RL) could be calculated
6 based on the above measured electromagnetic parameters using the following equations.

$$7 \quad RL = 20 \log \left| \frac{Z_{in} - 1}{Z_{in} + 1} \right| \quad (9)$$

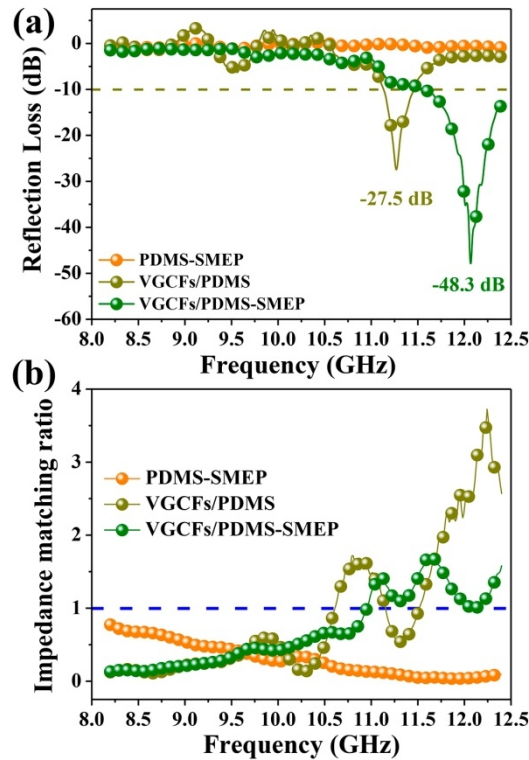
8 The normalized input impedance (Z_{in}) is calculated by the equation:

$$9 \quad Z_{in} = \sqrt{\frac{\mu_r}{\epsilon_r}} \tanh \left[j \left(\frac{2\pi f d}{c} \right) \sqrt{\mu_r \epsilon_r} \right] \quad (10)$$

10 Where, f is the frequency of incident wave and d is the thickness of the absorber; c is the
11 velocity of light electromagnetic waves in free space.

12 In Fig. 5a, the MA property of composites reaches -48.3 dB at 12.0 GHz with the
13 thickness of 7.2 mm. In addition, VGCFs/PDMS exhibits enhanced MA performance with
14 the RL_{min} values of -27.5 dB at 11.3 GHz, revealing that the addition of VGCFs in PDMS
15 plays a salient role in enhancement in dielectric loss and MA properties of the composites
16 [29]. It should be pointed out that wave-transparent SMEP was hybridized with

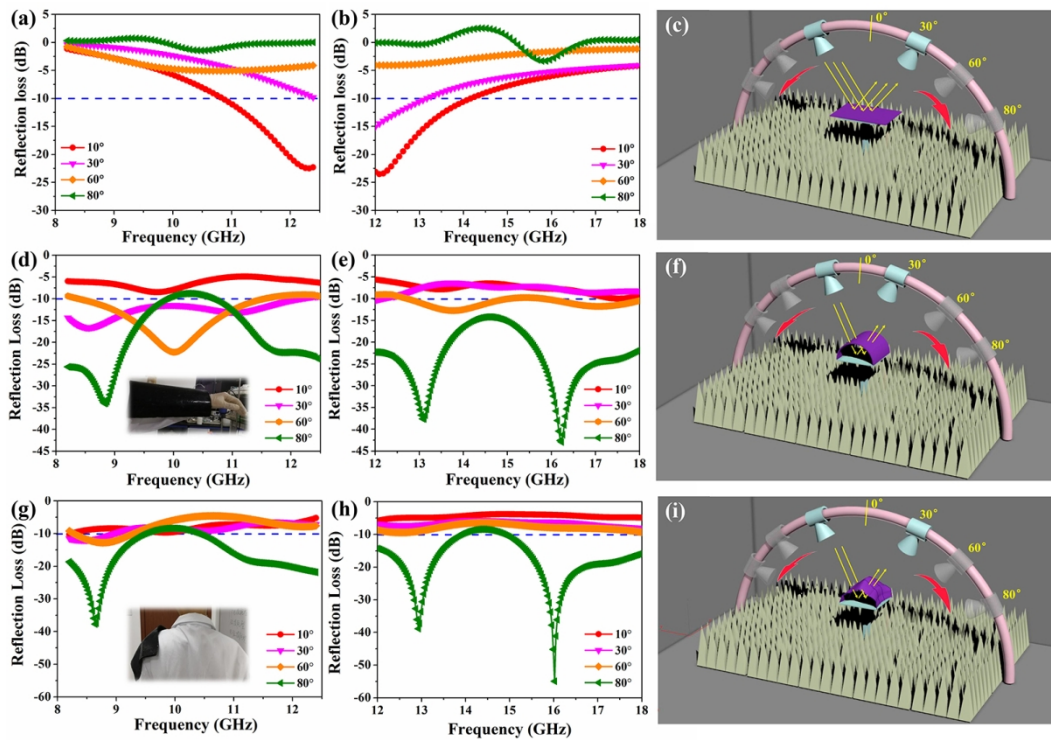
1 VGCFs/PDMS, thus forming sandwich-like absorption structure, inside which the incident
 2 microwave can be efficiently consumed in form of multiple reflections [4]. Impedance
 3 matching ratios Z ($|Z_{in}/Z_0|$) of specimens are calculated and shown in Fig. 5b. It is clear that
 4 the RL peak of VGCFs/PDMS-SMEP composites is in good accordance with the peak of
 5 impedance matching ratio curve, which is comparatively stable and closer to 1. These results
 6 implying that microwaves favorably propagate into the composites instead of being reflected,
 7 thus resulting in enhanced MA properties.



8
 9 **Fig. 5.** (a) Calculated reflection loss values, (b) impedance matching ratio of PDMS-SMEP,
 10 VGCFs/PDMS, and VGCFs/PDMS-SMEP at the thickness of 7.2 mm (filler loading of 10 wt%
 11 of VGCFs).

12 The assessment of practical MA abilities of VGCFs/PDMS-SMEP composites are
 13 performed and illustrated in Fig. 6. As shown in Fig. 4a and b, the RL_{min} of the composites
 14 with flat deformation reaches -23.5 dB (12.1 GHz) at the thickness of 2.0 mm at the incident

1 wave angle of 10° . Whereas, the RL_{min} values are decreased with the incident wave angle
 2 increase. Furthermore, comparing with flat deformation, it is worth noting that the RL_{min}
 3 values of arch-like-deformed composites are obviously increased with the increased incident
 4 microwave angle (Fig. 6d–f). For the incident microwave angle of 80° , the composites
 5 possess multiple band microwave absorption properties with the RL_{min} values of -34.0 dB, $-$
 6 37.4 dB, and -42.7 dB at 8.8 GHz, 13.1 GHz, and 16.2 GHz, respectively. In addition, after
 7 propelling the composites toward irregular deformation, the robust microwave absorption
 8 abilities of the composites are significantly boosted to -39.0 dB, -40.4 dB, and -55.7 dB at
 9 8.6 GHz, 12.9 GHz, and 16.0 GHz, respectively, where the absorption peaks slightly shifted
 10 0.2 GHz to the low frequency (Fig. 6g–i). Hence, VGCFs/PDMS–SMEP composites with
 11 different deformations have potential to be used in precious devices, where flexible and shape
 12 diversity are requested.

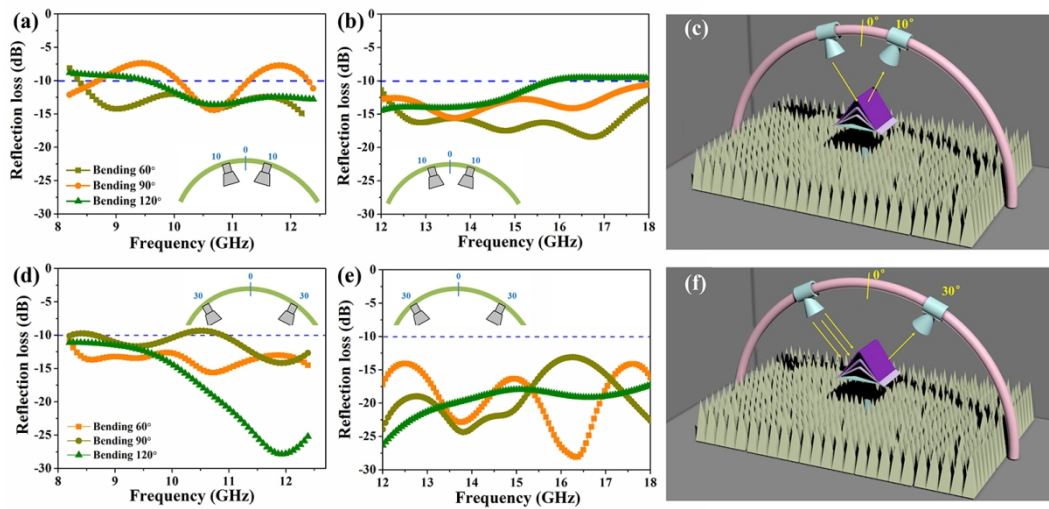


13
 14 **Fig. 6.** (a, b) RL curves, (c) schematically illustration of measurement mechanism for

1 VGCFs/PDMS–SMEP composites with flat deformation under varying measurement angles
2 (from 10 to 80°). (d, e) *RL* curves, (f) measurement mechanism of VGCFs/PDMS–SMEP
3 composites with arch-like deformation under varying measurement angles. (g, h) *RL* curves,
4 (i) measurement mechanism of VGCFs/PDMS–SMEP composites with irregular deformation
5 under varying measurement angles.

6 Based on the aforementioned results, the MA ability of VGCFs/PDMS–SMEP composites
7 is enhanced after propelling the composites toward irregular deformation. For further
8 analyzing the deformation effect of SMEP on MA properties, the VGCFs/PDMS–SMEP
9 composites is deformed in regular shape with the bending angle from 120° to 60°. As shown
10 in Fig. 7a, and b, the incident microwave angle was set as 10° to evaluate the practical MA
11 performance of different deformed VGCFs/PDMS–SMEP composites. The as–fabricated
12 composites maintain an EAB larger than 9.7 GHz (8.3–18.0 GHz) when the bending angle at
13 60°. Moreover, the EAB is regularly decreased with the increase of bending angles.
14 Meanwhile, when the incident wave angle is fixed as 30° (Fig. 7d–f), it is observed that the
15 composites hold the adjustable MA intensity, where the RL_{min} peaks are regularly shafted by
16 controlling bending angle from 60° to 120°. The RL_{min} value reaches –28.1 dB at 12.0 GHz
17 with the bending angle of 120°. Broadband MA performance is clearly observed with the
18 EAB covered the frequency range of 9.8 GHz (8.2–18.0 GHz). Thus, owing to the effective
19 dielectric loss property and sandwich–like structure, as–prepared composites possess
20 sustainable broadband MA ability. More importantly, the MA intensity can be intelligently
21 regulated via controlling the different permanent deformation of VGCFs/PDMS–SMEP
22 composites, resulted from the superior shape memory capability of SMEP [2,30]. Hence,

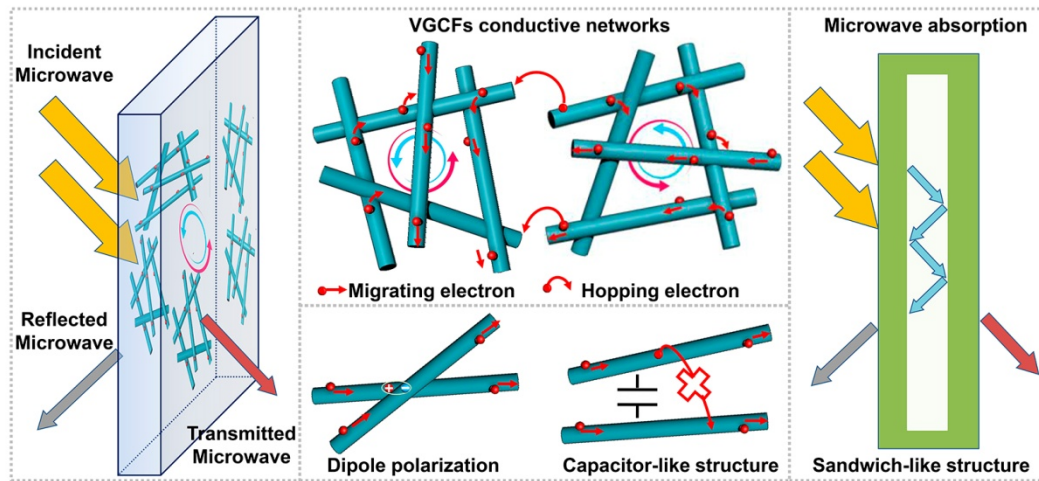
1 according to the frequency of incident electromagnetic waves, the VGCFs/PDMS–SMEP
 2 composites can be utilized as intelligent MAMs to absorb the adverse and complex
 3 electromagnetic waves radiation by programming the deformation of composites under
 4 thermal stimuli.



5
 6 **Fig. 7.** (a, b) *RL* curves, (c) schematically illustration of measurement mechanism for
 7 VGCFs/PDMS–SMEP composites with varying bending deformation at incident microwave
 8 angle of 10°. (d, e) *RL* curves, (f) measurement mechanism for VGCFs/PDMS–SMEP
 9 composites with varying bending deformation at incident microwave angle of 30°.

10 Based on the above analysis, a probable microwave absorption mechanism is proposed in
 11 Fig. 8. Owing to the addition of VGCFs, VGCFs/PDMS–SMEP composites possess
 12 enhanced conductivity loss, dielectric loss and impedance matching performance, which
 13 result in the enhanced microwave absorption performance. For dielectric loss, it can be
 14 deeply analyzed by electronic transport modes existed in VGCFs/PDMS composites,
 15 involving the migration and hopping of electrons [6]. The migrating electrons endow the
 16 VGCFs/PDMS–SMEP composites with high conductivity, coupling with enhancing the
 17 dipole polarization between VGCFs. The hopping electrons could enhance the micro-current

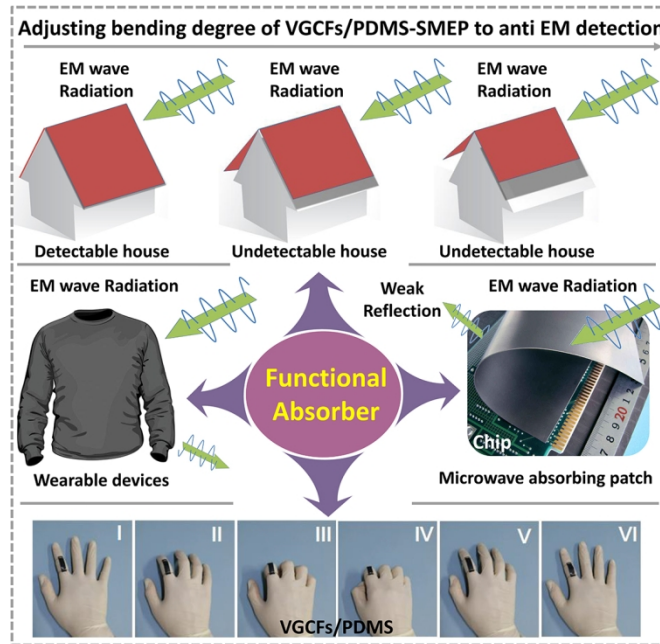
1 in the VGCFs network, which provides excellent dielectric loss. In addition, the non-
 2 conductive network of VGCFs lead to the formation of capacitor-like structures at the
 3 interfaces between VGCFs and PDMS matrix. The capacitor-like structures performed as
 4 conductivity loss may attenuate the intensity of incident microwaves [12]. Moreover, the
 5 sandwich-like structure enabled by wave-transparent SMEP favors the multiple reflection of
 6 incident microwave. Finally, the incident microwave can be efficiently absorbed and
 7 converted into thermal or other forms of energy [27].



8
 9 **Fig. 8.** Possible microwave absorption mechanism of VGCFs/PDMS-SMEP composites.

10 Based on above analysis, VGCFs/PDMS-SMEP composites is expected to be used as
 11 functional building materials for practical applications, where shape memory, intelligent
 12 absorption frequency regulation, and multi-functional absorbers are required. As shown in
 13 Fig. S4, VGCFs/PDMS-SMEP composites shows the maximum tensile stress of 40.0 MPa at
 14 the strain of 13.8%. At mean time, the SMEP layer in the composites is fractured, resulting in
 15 interfaces separation and sharp decrease of tensile stress. With the continued stretching of
 16 VGCFs/PDMS, the composites is completely fractured at the maximum tensile strain of
 17 103%. Moreover, VGCFs/PDMS also possesses expected microwave absorption capabilities,

1 as well as superior mechanical property. VGCFs/PDMS composites can be simply stretched
 2 several times to its initial state, which the corresponding strain–stress curve is shown in Fig.
 3 S5. Due to the cross–linked networks of O–Si–O and the enhancement of VGCFs,
 4 VGCFs/PDMS own enough flexibility with maximum tensile strain of 640% at tensile stress
 5 of 1.8 MPa. Thus, VGCFs/PDMS is potential to design of “wearable” absorbers for
 6 equipment and human beings. Therefore, our fabricated composites are expected to be used
 7 as multi–functional absorbers in wearable electronic devices, chips protection, and stealth
 8 technology (Fig. 9) [31].



9
 10 **Fig. 9.** Illustration of representative properties for the multi–functional broadband shape
 11 memory absorber.

12 **4. Conclusion**

13 In conclusion, we describe an intelligent microwave absorption technology using
 14 VGCFs/PDMS–SMEP as absorber. The VGCFs/PDMS–SMEP composites delivers smart
 15 tunable microwave absorption capability, where the RL_{min} peaks are regularly shafted by

1 morphing the composites deformation. The RL_{min} value reaches -55.7 dB at 16.0 GHz with
2 the thickness of 2.0 mm under a manipulated irregular arch-like deformation. While, the EAB
3 is also reaches 9.8 GHz, which covered whole applied microwave frequency (8.2–18.0 GHz).
4 Such a smart microwave absorber is enabled by superior shape memory effect of SMEP,
5 conductivity loss and dielectric loss properties of VGCFs/PDMS, and well-constructed
6 sandwich-like structure. The dielectric loss performance of the composites is enhanced by
7 the dipole relaxation in form of migration and hopping of electrons between VGCFs.
8 Therefore, the VGCFs/PDMS–SMEP composites serves as the key that really opens up
9 opportunity for the application in wearable devices, chips protection, and information
10 security.

11

12 **Conflicts of interest**

13 There are no conflicts to declare.

14

15 **Acknowledgements**

16 This work was supported by the Natural Science Foundation of Zhejiang Province, China
17 (Grant No. LY19E030009), the National Natural Science Foundation of China (NSFC)
18 (Grant No. 51503183), Key Program for International Science and Technology Cooperation
19 Projects of Ministry of Science and Technology of China (No. 2016YFE0125900), the
20 Fundamental Research Funds of Zhejiang Sci-Tech University (Grant No. 2019Q009) and
21 the Engineering and Physical Sciences Research Council (EPSRC) grant-EP/N007921.

22 **Appendix A. Supplementary data**

1 Supplementary data to this article can be found online: .

References

- [1] Menon AV, Madras G, Bose S, Shape memory polyurethane nanocomposites with porous architectures for enhanced microwave shielding. *Chem Eng J* 2018;352:590–600.
- [2] Wang HG, Meng FB, Huang F, Jing CF, Li Y, Wei W, Zhou ZW, Interface modulating CNTs@PANi hybrids by controlled unzipping the walls of CNTs to achieve tunable high-performance microwave absorption. *ACS Appl Mater Interfaces* 2019;11:12424-12153.
- [3] Ye F, Song Q, Zhang Z, Li W, Zhang S, Yin X, Zhou Y, Tao H, Liu Y, Cheng L, Zhang L, Li H, Direct Growth of Edge-Rich Graphene with Tunable Dielectric Properties in Porous Si₃N₄ Ceramic for Broadband High-Performance Microwave Absorption. *Adv Funct Mater* 2018;28:1707205.
- [4] Yan Y, Xia H, Qiu Y, Xu Z, Ni Q, Fabrication of gradient vapor grown carbon fiber based polyurethane foam for shape memory driven microwave shielding. *RSC Adv* 2019;9:9401–9409.
- [5] Singh BP, Saket DK, Singh AP, Pati S, Gupta TK, Singh VN, Dhakate SR, Dhawan SK, Kotnala RK, Mathur RB, Microwave shielding properties of Co/Ni attached to single walled carbon nanotubes. *J Mater Chem A* 2015;3:13203–13209.
- [6] Zhang Y, Wang X, Cao M, Confinedly implanted NiFe₂O₄-rGO: Cluster tailoring and highly tunable electromagnetic properties for selective-frequency microwave absorption. *Nano Res* 2018;11:1426–1436.
- [7] Wang HG, Meng FB, Li JY, Li T, Chen ZJ, Luo HB, Zhou ZW, Carbonized design of hierarchical porous carbon/Fe₃O₄@Fe derived from loofah sponge to achieve tunable high-performance microwave absorption, *ACS Sustain Chem Eng* 2018;6:11801-11810.
- [8] Lv H, Yang Z, Wang PL, Ji G, Song J, Zheng L, Zeng H, Xu ZJ, A Voltage-Boosting Strategy Enabling a Low-Frequency, Flexible Electromagnetic Wave Absorption Device. *Adv Mater* 2018;30:e1706343.
- [9] Sun H, Che R, You X, Jiang Y, Yang Z, Deng J, Qiu L, Peng H, Cross-stacking aligned carbon-nanotube films to tune microwave absorption frequencies and increase absorption intensities. *Adv Mater* 2014;26:8120–8125.
- [10] Yu L, Yang Q, Liao J, Zhu Y, Li X, Yang W, Fu Y, A novel 3D silver nanowires@polypyrrole sponge loaded with water giving excellent microwave absorption properties. *Chem Eng J* 2018;352:490–500.
- [11] Zhang Y, Huang Y, Zhang T, Chang H, Xiao P, Chen H, Huang Z, Chen Y, Broadband and tunable high-performance microwave absorption of an ultralight and highly compressible graphene foam. *Adv Mater* 2015;27:2049–2053.

- 1
2 [12] Ma J, Wang X, Cao W, Han C, Yang H, Yuan J, Cao M, A facile fabrication and highly tunable
3 microwave absorption of 3D flower-like Co_3O_4 -rGO hybrid-architectures. *Chem Eng J*
4 2018;339:487–498.
- 5 [13] Leng J, Lan X, Liu Y, Du S, Shape-memory polymers and their composites: Stimulus methods and
6 applications. *Prog Mater Sci* 2011;56:1077–1135.
- 7 [14] Xu B, Zhang L, Pei YT, Luo JK, Tao SW, De Hosson JTM., Fu YQ, Electro-Responsive Polystyrene
8 Shape Memory Polymer Nanocomposites. *Nanosci Nanotech Lett* 2012;4:814–820.
- 9 [15] Yan Y, Xia H, Qiu Y, Xu Z, Ni QQ, Shape memory driving thickness-adjustable G@SMPU sponge
10 with ultrahigh carbon loading ratio for excellent microwave shielding performance. *Mater Lett*
11 2019;236:116–119.
- 12 [16] Wang E, Dong Y, Islam MDZ, Yu L, Liu F, Chen S, Qi X, Zhu Y, Fu Y, Xu Z, Hu N, Effect of
13 graphene oxide-carbon nanotube hybrid filler on the mechanical property and thermal response speed
14 of shape memory epoxy composites. *Compos Sci Technol* 2019;169:209–216.
- 15 [17] Lu H, Liu Y, Xu BB, Hui D, Fu YQ, Spontaneous biaxial pattern generation and autonomous wetting
16 switching on the surface of gold/shape memory polystyrene bilayer. *Compos Part B* 2017;122:9–15.
- 17 [18] Yan Y, Xia H, Qiu Y, Xu Z, Ni QQ, Highly aligned nonwoven vapor grown carbon fibre based
18 polyurethane fibrous membrane for direction-dependent microwave shielding. *Mater Lett*
19 2019;245:98–102.
- 20 [19] Liu Y, Wang X, Feng S, Nonflammable and Magnetic Sponge Decorated with Polydimethylsiloxane
21 Brush for Multitasking and Highly Efficient Oil-Water Separation. *Adv Funct Mater*
22 2019;29:1902488.
- 23 [20] Chu K, Yun DJ, Kim D, Park H, Park SH, Study of electric heating effects on carbon nanotube
24 polymer composites. *Org Electron* 2014;15:2734–2741.
- 25 [21] Shang S, Gan L, Yuen MCW, Jiang SX, Mei Luo N, Carbon nanotubes based high temperature
26 vulcanized silicone rubber nanocomposite with excellent elasticity and electrical properties. *Compos*
27 *Part A* 2014;66:135–141.
- 28 [22] Rahmani S, Mortaheb HR, Omidkhah MR, Khodadadi Dizaji A, Investigation on Performance of
29 PDMS-Graphene/PES Hybrid Membrane for Pervaporative Separation of Phenol from Aqueous
30 Streams. *Polym-Plast Tech Mater* 2018;58:305–315.
- 31 [23] Gao Y, Liu W, Zhu S, Polyolefin Thermoplastics for Multiple Shape and Reversible Shape Memory.
ACS Appl Mater Interfaces 2017;9:4882–4889.

- 1 [24] Wang E, Wu Y, Islam MZ, Dong Y, Zhu Y, Liu F, Fu Y, Xu Z, Hu N, A novel reduced graphene
2 oxide/epoxy sandwich structure composite film with thermo-, electro- and light-responsive shape
3 memory effect. *Mater Lett* 2019;238:54–57.
- 4 [25] Xu B, Fu YQ, Huang WM, Pei YT, Chen ZG, De Hosson JTM, Kraft A, Reuben RL, Thermal–
5 Mechanical Properties of Polyurethane-Clay Shape Memory Polymer Nanocomposites. *Polymers*
6 2010;2:31–39.
- 7 [26] Wang W, Lu H, Liu Y, Leng J, Sodium dodecyl sulfate/epoxy composite: water-induced shape
8 memory effect and its mechanism. *J Mater Chem A* 2014;2:5441.
- 9 [27] Li X, Yu L, Yu L, Dong Y, Gao Q, Yang Q, Yang W, Zhu Y, Fu Y, Chiral polyaniline with
10 superhelical structures for enhancement in microwave absorption. *Chem Eng J* 2018;352:745–755.
- 11 [28] Li X, Yu L, Zhao W, Shi Y, Yu L, Dong Y, Zhu Y, Fu Y, Liu X, Fu F, Prism-shaped hollow carbon
12 decorated with polyaniline for microwave absorption. *Chem Eng J* 2020;379:122393.
- 13 [29] Meng F, Wang H, Wei, Chen Z, Li T, Li C, Xuan Y, Zhou Z, Generation of graphene-based aerogel
14 microspheres for broadband and tunable high-performance microwave absorption by electrospinning–
15 freeze drying process. *Nano Res* 2018;11:2847–2861.
- 16 [30] Song WL, Zhou Z, Wang LC, Cheng XD, Chen M, He R, Chen H, Yang Y, Fang D, Constructing
17 Repairable Meta-Structures of Ultra-Broad-Band Electromagnetic Absorption from Three–
18 Dimensional Printed Patterned Shells. *ACS Appl Mater Interfaces* 2017;9:43179–43187.
- 19 [31] Zhang KL, Zhang JY, Hou ZL, Bi S, Zhao QL, Multifunctional broadband microwave absorption of
20 flexible graphene composites. *Carbon* 2019;141:608–617.

Declaration of interests

The authors declare that they have no known competing financial interests or personal relationships that could have appeared to influence the work reported in this paper.

The authors declare the following financial interests/personal relationships which may be considered as potential competing interests:

Author Statement

Li Xiang: Conceptualization, Methodology, Writing-Original Draft.

Zhu Yaofeng: Writing-Review & Editing, Supervision, Funding acquisition.

Liu Xuqing: Writing-Review & Editing, Resources.

Xu Ben Bin: Writing-Review & Editing, Funding acquisition.

Ni Qingqing: Resources.

A broadband and tunable microwave absorption technology enabled by VGCFs/PDMS–EP shape memory composites

Xiang Li^a, Yaofeng Zhu^{a*}, Xuqing Liu^b, Ben Bin Xu^{c*}, Qingqing Ni^d

^a *Key Laboratory of Advanced Textile Materials and Manufacturing Technology of Ministry of Education, Zhejiang Sci-Tech University, No. 928 Second Avenue Xiasha Higher Education Zone, Hangzhou, 310018, Zhejiang, P.R. China*

^b *School of Materials, University of Manchester, Oxford Road, Manchester, United Kingdom, M13 9PL*

^c *Department of Mechanical and Construction Engineering, Northumbria University, Newcastle upon Tyne, United Kingdom, NE1 8ST*

^d *Interdisciplinary Graduate School of Science and Technology, Shinshu University, Tokida, Ueda, 386-8576, Japan*

*Corresponding authors.

Email addresses: yfzhu@zstu.edu.cn (Y. Zhu), ben.xu@northumbria.ac.uk (B. Xu).

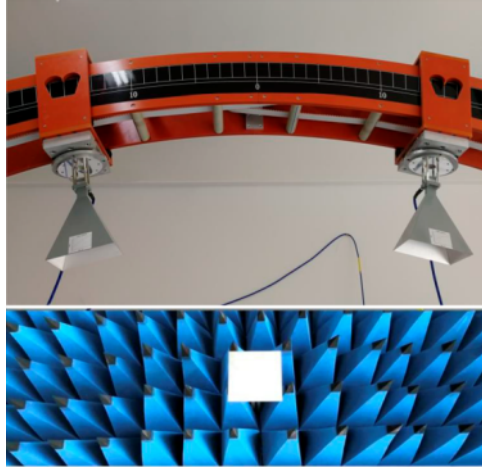


Fig. S1. Photographs of arch method measurement.

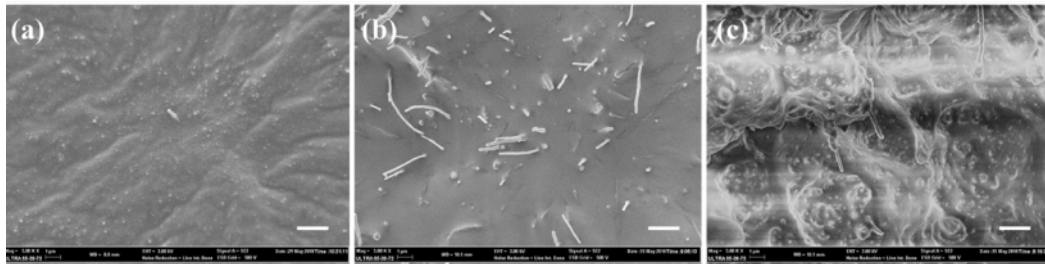


Fig. S2. FE-SEM images of VGCFs/PDMS hybrids with VGCFs loading (a) 2 g (5 wt%), (b) 4 g (10 wt%), and (c) 6g (15 wt%), scale bar is 2 μm .

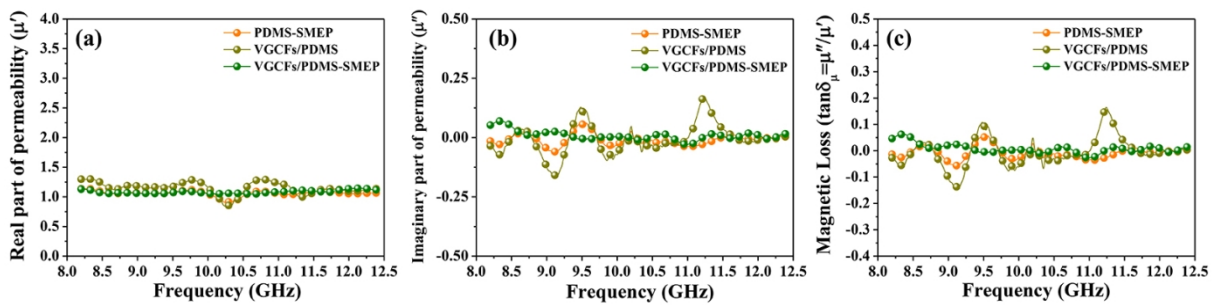


Fig. S3. (a) real part (μ') and (b) imaginary part (μ'') of complex permeability, and (c) magnetic loss values (μ''/μ') of PDMS-SMEP, VGCFs/PDMS and VGCFs/PDMS-SMEP.

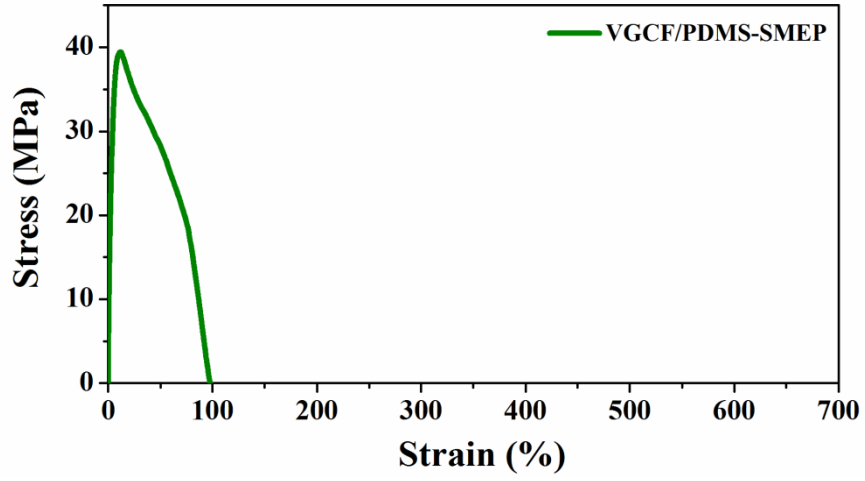


Fig. S4. Strain-stress curve of VGCFs/PDMS-SMEP.

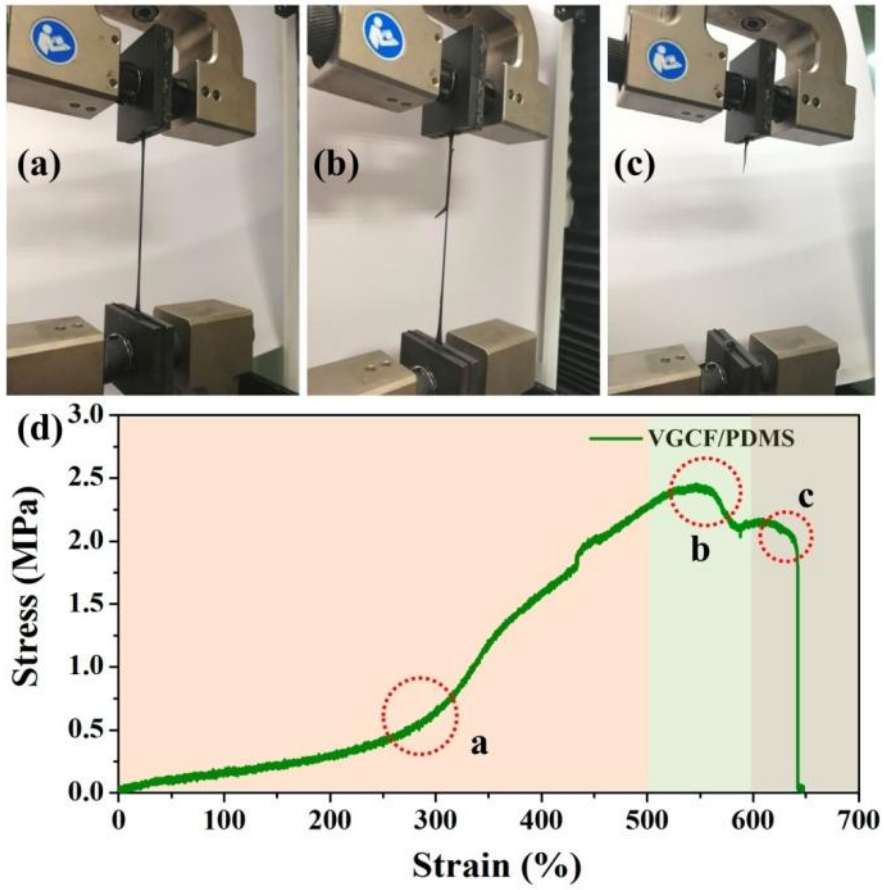


Fig. S5. (a, b, and c) tensile process of VGCFs/PDMS with stretching velocity of 10 mm/min, (d) strain-stress curve of VGCFs/PDMS.